D12

N84 15602

PROPAGATION OF FLEXURAL AND MEMBRANE WAVES WITH FLUID LOADED NASTRAN PLATE AND SHELL ELEMENTS

A. J. Kalinowski and C. A. Wagner

NAVAL UNDERWATER SYSTEMS CENTER
NEW LONDON, CONNECTICUT 06320

SUMMARY

This paper is concerned with modeling flexural and membrane type waves existing in various submerged (or in vacuo) plate and/or shell finite element models that are excited with steady state type harmonic loadings proportioned to $e^{i\omega t}$. Only thin walled plates and shells are treated wherein rotary inertia and shear correction factors are not included. More specifically, the issue of determining the shell or plate mesh size needed to represent the spatial distribution of the plate or shell response is of prime importance towards successfully representing the solution to the problem at hand. To this end, a procedure is presented for establishing guide lines for determining the mesh size based on a simple test model that can be used for a variety of plate and shell configurations such as, (1) cylindrical shells with water loading, (2) cylindrical shells in vacuo, (3) plates with water loading, and (4) plates in vacuo. The procedure for doing these four cases is given, with specific numerical examples present only for the cylindrical shell case.

INTRODUCTION

This paper addresses the topic of modeling flexural waves and membrane waves present in various types of shell and plate type structural configurations. The issue at hand is arriving at a simple procedure for determining a mesh size adequate to represent the details of the spatial response distributions necessary to achieve some desired level of accuracy. To be sure, it would be too large an undertaking to answer this question for all possible plate and shell configurations that may arise, however, the selected class of thin walled cylindrical shells and flat plates are often the major building blocks of a good deal of structures. Therefore, the paper will focus on these two configurations, with the major emphasis on the cylindrical shell employing CCONEAX elements with axisymmetrical loading. Physical problems with finite length dimensions exhibit solution responses that often have the form of standing wave patterns as a result of reflections from the shell boundaries. Further, these solutions do not have a single clearly defined constant amplitude traveling wave component as one would have, in say, an infinitely long

C-3

shell or plate. A constant amplitude traveling wave (propagating in the x direction at frequency ω) response, R, of the form $R = R_0 e^{i(-\gamma x+\omega t)}$ is a desirable form to seek because the constant amplitude R_0 and associated spatial wave length $\lambda_\gamma = 2\pi/\gamma$ can then be used as a measure for determining the ability of a particular element to represent the desired wave propagation phenomenon. Deviations of the finite element amplitude response from the exact response constant R_0 and/or deviatons of the finite element response phase angle period from the exact spatial period can be used to judge the mesh refinement necessary to achieve a desired level of accuracy. The thrust of this paper is not to give a hard and fast rule for the number of elements per wavelength necessary to achieve some desired level of accuracy, but rather to provide a procedure for allowing one to establish his own level of accuracy. We take this approach because rules of thumb are often dangerous, particularly in the area of wave propagation in plate and shell structures. There are cases, for example, in a plate or cylindrical shell where a cutoff point exists such that the particular problem parameters (geometry, frequency, and physical constants) result in a situation where there is no traveling wave. If the problem parameters happen to be such that the traveling wave root is close to the cut-off point, a finer mesh size might be needed to properly represent the propagating wave situation.

The symmetrically loaded (θ independent loading) infinitely long cylinder shell (with or without fluid external fluid present) is selected as the model for examining flexural and membrane traveling waves (see Figure 1). This same model can be used to treat all four plate and shell cases (with and without water) discussed above. The plate cases can be realized by letting $a \to \infty$ and the in vacuo cases achieved by setting the density of the fluid equal to zero.

SYMBOLS

a = radius of cylindrical shell (in)

c = fluid sound speed (in/sec)

c_s = shear velocity = $\sqrt{G/\rho_s}$ psi

c_p = in vacuo plate wave speed, $\sqrt{E/(\rho_s(1-\nu^2))}$ (in/sec)

c_γ = propagating wave phase velocity, ω/γ

c_{fp} = in vacuo plate wave speed, $\sqrt[4]{h\rho_s\omega^2/D}$ (in/sec)

D = plate modulus = $Eh^3/[12\ (1-\nu^2)]$ of rigidity (lb/in)

f = harmonic frequency (Hz)

G = shear modulus of elasticity (psi)

$H_0^{(1)}(\ )$; $H_1^{(1)}(\ )$ = Hankel Bessel functions of the first kind order 0 and 1

h = plate or shell thickness (in)

i = $\sqrt{-1}$ complex number

$K_0()$; $K_1()$ = modified Bessel functions of order 0 and 1

k = ω/c acoustic wave number (in^{-1})

k_{fp} = ω/c_{fp} in vacuo plate wave number (in^{-1})

k_p = ω/c_p in vacuo plate wave number (in^{-1})

L = finite element model length (in)

M_z = shell line moment (lb/in/in)

N_z = axial line membrane force (lb/in)

p = fluid pressure (psi)

Q = transverse shell line shear force (lb/in)

r = radial cylindrical coordinate (in)

t = time variable (sec)

u = axial motion of plate or shell (in)

U_o = amplitude of u (in)

w = radial motion of plate or shell (in)

W_o = amplitude of w (in)

x = plate coordinate direction normal to plate (in)

z = axial cylindrical coordinate variable (in)

λ_γ = wavelength of propagating wave

γ = traveling wave number for z direction (in^{-1})

γ_r = real part of γ

γ_i = imaginary part of γ

ρ = mass density of fluid ($lb/sec^2\ in^{-4}$)

ρ_s = mass density ofstructure ($lb/sec^2\ in^{-4}$)

ν = Poisson's ratio of structure

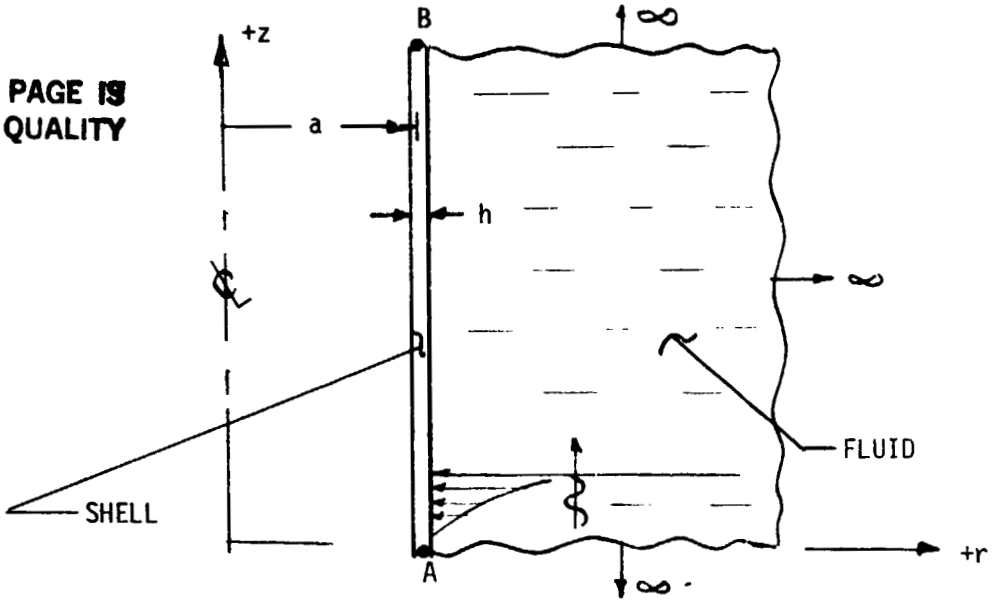

FIGURE 1. FLEXURAL WAVE MODEL FOR SUBMERGED CYLINDRICAL SHELL

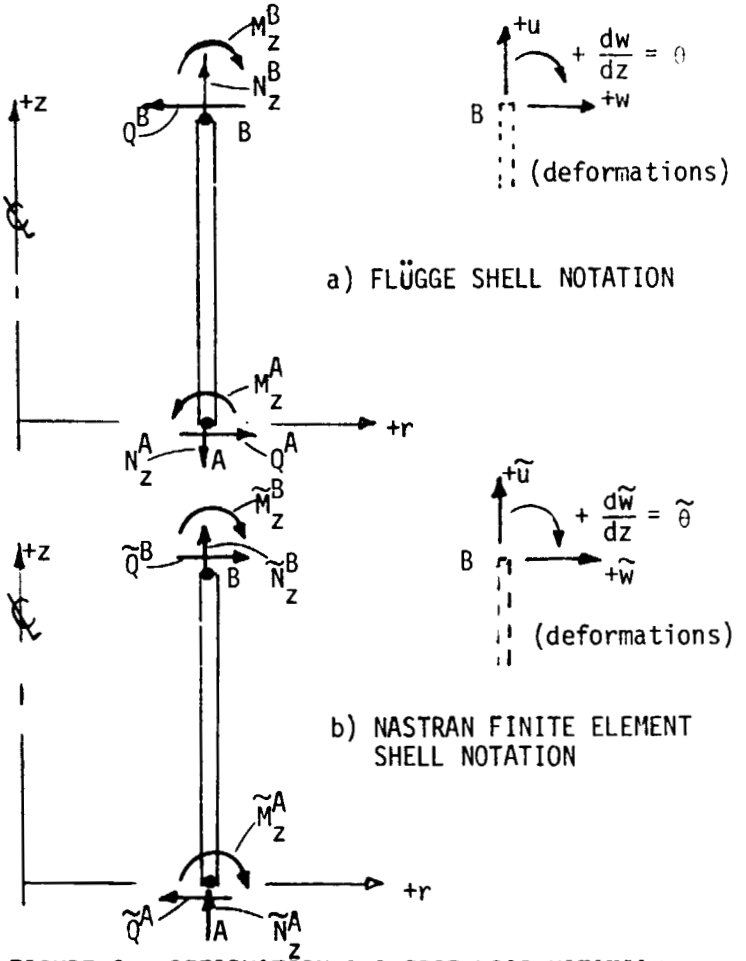

FIGURE 2. DEFORMATION AND EDGE LOAD NOTATION

$\omega = 2\pi f$ = harmonic frequency (rad/sec)

ANALYTICAL WAVELENGTH FORMULATION FOR PLATES AND CYLINDRICAL SHELLS

The analytical formulation employed for determining the exact relationship for freely propagating waves in plate and cylindrical shell structures is important for its own sake, however, the formulation also directly leads to the procedure employed to set up the NASTRAN wavelength accuracy demonstration models. Consequently, some of the important details of the development for the freely propagating wave characteristics equation are given. The procedure given will closely follow the one given in ref. 2, except that freely propagating rather than standing wave configurations are considered by changing the axial variation as a complex exponential variation in z rather than a cosine variation.

Of eventual interest is both the flexural wave and axial (membrane) wavelengths for plates (with and without water present) and for infinitely long cylindrical shells (with and without water present). This constitutes 2 x 2 x 2 = 8 different situations. However, we can treat the eight cases at the same time by first treating the most complex case of the submerged infinitely cylindrical shell. By taking appropriate limits of this case (i.e., water density $\to 0$ or shell radius $\to \infty$) we can recover the other cases of interest without requiring any new analyses.

We start with the governing simplified thin wall shell field equations for the cylindrical shell (ref. 1) and corresponding wave equation for the external fluid, namely

$$\frac{\partial^2 u}{\partial z^2} + \frac{\nu}{a}\frac{\partial w}{\partial z} - \frac{\partial^2 u}{\partial t^2} \cdot \frac{1}{c_p^2} = 0 \tag{1}$$

$$\frac{\nu}{a}\frac{\partial u}{\partial z} + \frac{w}{a^2} + \frac{h^2}{12}\frac{\partial^4 w}{\partial z^4} + \frac{\partial^2 w}{\partial t^2} \cdot \frac{1}{c_p^2} = -\,p\Big|_{r=a} \cdot (1-\nu^2)/(Eh)$$

$$\nabla^2 p - \frac{1}{c^2}\frac{\partial^2 p}{\partial t^2} = 0 \tag{2}$$

subject to the usual boundary condition relation relating the pressure gradient normal to the shell and the shell acceleration,

$$\frac{\partial p}{\partial r}\Big|_{r=a} = -\rho\frac{\partial^2 w}{\partial t^2} \tag{3}$$

where u, w are the axial, and radial displacements of the shell (see Figure 2a for positive sense); p is the pressure in the fluid; h the shell thickness; a the radius of the cylindrical shell; r, z are the radial axial cylindrical coordinates; E, ν are Young's modulus and Poisson's ratio of the shell; c_p is the plate wave speed parameter ($\sqrt{E/(\rho_s(1-\nu^2))}$); and c is the acoustic wave

speed of the fluid. The shell equations (1) are for classical thin wall plate and shell theory and do not have rotary inertia and shear correction factors included. Consequently, the area of interest focused on herein will be in a frequency range of ω such that the above two methods correction factors are not necessary. This point will be expanded upon later in the paper.

The θ symmetrical shell motion representing propagating waves in the $+z$ direction are assumed to take the form

$$\begin{aligned} u &= U_o\, e^{i\gamma z}\, e^{-i\omega t} \\ v &= 0 \qquad \text{(no hoop motion)} \\ w &= W_o\, e^{i\gamma z}\, e^{-i\omega t} \end{aligned} \tag{4}$$

where U_o and W_o are the yet to be determined wave amplitudes, and γ is the propagating wave number. For outward going waves, the form of the pressure solution identically satisfying the wave equation (2) is given by ref. 2,

$$p(r,z) = P_o\, H_o^{(1)}(r\sqrt{k^2-\gamma^2})e^{i\gamma z}\, e^{-i\omega t} \tag{5}$$

which can be easily verified by direct substitution of equation (5) into equation (2), where P_o is the yet unknown pressure amplitude, and $H_o^{(1)}(\,)$ is the Hankel function of the first kind of order zero. A similar expression for p with $H_o^{(2)}(\,)$ (Hankel functions of the second kind) also satisfies the wave equation, but represents inward coming waves (when $k^2 > \gamma^2$) or results in an ever increasing exponential increasing pressure field with increasing r when $k^2 < \gamma^2$. Neither of these situations corresponds to the physical problem at hand, thus only the Hankel function of the first kind is retained.

The characteristic equation resulting in an interaction equation relating the driving frequency ω and admissible propagating wave numbers, γ, is obtained by substituting equations (4) and (5) into equation (1), subject to the boundary condition (3): actually substituting equations (4) and (5) into condition (3) leads to the relation between the surface motion amplitude W_o and the pressure amplitude P_o, namely

$$P_o = \frac{-\rho\, W_o\, \omega^2}{\sqrt{k^2-\gamma^2}\; H_1^{(1)}\,(a\sqrt{k^2-\gamma^2})}. \tag{5a}$$

Thus the resulting two linear equations in the W_o, U_o coefficients is given by

$$\begin{aligned} &U_o\, i\left(\frac{\omega^2}{c_p^2} - \gamma^2\right) + W_o\left(-\frac{\nu\gamma}{a}\right) = 0 \qquad (6) \\ &U_o\, i\left(\frac{\nu\gamma}{a}\right) + W_o\left[\frac{1}{a^2} + \frac{h^2}{12}\gamma^4 - (\omega/c_p)^2 - \frac{(1-\nu^2)\rho\omega^2 H_o^{(1)}\,(a\sqrt{k^2-\gamma^2})}{Eh\sqrt{k^2-\gamma^2}\; H_1^{(1)}\,(a\sqrt{k^2-\gamma^2})}\right] = 0 \end{aligned}$$

The nontrivial solution is obtained by setting the determinant of the amplitude coefficients equal to zero resulting in

$$\left(\frac{\omega^2}{c_p^2} - \gamma^2\right)\left[\frac{1}{a^2} + \frac{h^2}{12}\gamma^4 - (\omega/c_p)^2 - \frac{(1-\nu^2)\rho\omega^2 H_o^{(1)}\,(a\sqrt{k^2-\gamma^2})}{Eh\sqrt{k^2-\gamma^2}\; H_1^{(1)}\,(a\sqrt{k^2-\gamma^2})}\right] + \left(\frac{\nu\gamma}{a}\right)^2 = 0 \tag{7a}$$

for $k^2 > \gamma^2$

or in another equivalent form of

$$\left(\frac{\omega^2}{c_p^2} - \gamma^2\right)\left[\frac{1}{a^2} + \frac{h^2}{12}\gamma^4 - (\omega/c_p)^2 - \frac{(1-\nu^2)\rho\omega^2 K_0(a\sqrt{\gamma^2-k^2})}{Eh\sqrt{\gamma^2-k^2}\ K_1(a\sqrt{\gamma^2-k^2})}\right] + \left(\frac{\nu\gamma}{a}\right)^2 = 0 \tag{7b}$$

for $\gamma^2 > k^2$

where the $K_0()$ and $K_1()$ are modified Bessel functions and are related to the Hankel functions by the identity

$$K_n(X) = \frac{\pi}{2} i^{n+1} H_n^{(1)}(iX) \tag{8}$$

Noting that the in vacuo flexural wave number, k_{fp}, formula for a plate is given by

$$k_{fp} = \sqrt[4]{\frac{h\rho_s\omega^2}{D}} \tag{9}$$

and the in vacuo membrane compressional wave number, k_p, given by

$$k_p = \frac{\omega}{c_p} = \frac{\omega}{\sqrt{\frac{E}{(1-\nu^2)\rho_s}}} \tag{10}$$

and finally the acoustic wave number by

$$k = \frac{\omega}{c} \tag{11}$$

where c is the acoustic wave speed of the fluid medium; the characteristic equation for the traveling wave number, non-dimensionalized with respect to the acoustic wave number k, can algebraically be rewritten as

$$\left((k_p/k)^2-(\gamma/k)^2\right)\left[\frac{1}{(ka)^2} - \left(\frac{k_p}{k}\right)^2\left\{1 - \frac{(\gamma/k)^4}{(k_{fp}/k)^4} + \frac{\left(\frac{\rho a}{\rho_s h}\right) H_0^{(1)}(ka\sqrt{1-\left(\frac{\gamma}{k}\right)^2})}{(ka)\sqrt{1-\left(\frac{\gamma}{k}\right)^2}\ H_1^{(1)}(ka\sqrt{1-\left(\frac{\gamma}{k}\right)^2})}\right\}\right]$$

$$+ \frac{\nu^2(\gamma/k)^2}{(ka)^2} = 0 \tag{12a}$$

$$\text{For } \left(\frac{\gamma}{k}\right)^2 < 1$$

or

$$\left((k_p/k)^2-(\gamma/k)^2\right)\left[\frac{1}{(ka)^2} - \left(\frac{k_p}{k}\right)^2\left\{1 - \frac{(\gamma/k)^4}{(k_{fp}/k)^4} + \frac{\frac{\rho a}{\rho_s h} K_0(ka\sqrt{\left(\frac{\gamma}{k}\right)^2-1})}{ka\sqrt{\left(\frac{\gamma}{k}\right)^2-1}\ K_1(ka\sqrt{\left(\frac{\gamma}{k}\right)^2-1})}\right\}\right]$$

$$+ \frac{\nu^2(\gamma/k)^2}{(ka)^2} = 0 \tag{12b}$$

$$\text{For} \left(\frac{\gamma}{k}\right)^2 > 1$$

The original dimensional form of the characteristic equation (7) depended on the eight parameters h, ω, E, ν, ρ, ρ_s, a, c, for the resulting wave number γ; however, the above equation (12) form only depends on the reduced number of 5 non-dimensional parameters, namely k_p/k, ka, ρ/ρ_s, a/h, and ν for the resulting non-dimensional wave numbers γ/k. The term (k_{fp}/k) is not an independent parameter since it can be expressed in terms of the other ones through the relation

$$\frac{k_{fp}}{k} = (12)^{\frac{1}{4}} \sqrt{(k_p/k)\left(\frac{a}{h}\right)}/(ka)^{\frac{1}{2}} \tag{13}$$

Roots of Characteristic Equation and Mode Shapes

The roots of the frequency equation (12) cover several special cases and require further elaboration. The roots of interest for freely propagating waves are those for which $\gamma = \gamma_r$ is a real quantity, wherein the shell response has arguments (see equation (4)) of the traveling wave form $i(\gamma_r z - \omega t)$ and corresponds to a wave propagating in the +z direction and the corresponding wavelength is given by

$$\lambda = \frac{2\pi}{\gamma_r} \tag{14}$$

Possibly roots of the characteristic equation are complex (e.g., this could be the case when employing equation (12a) due to the complex form of the Hankel functions $H_n(\ ) = J_n(\ ) + i\, Y_n(\ ))$. In these situations, the complex root can be written in the form $\gamma = \gamma_r + i\gamma_i$ and substitution of this quantity into the shell response equation (4), shows that the axial z response is proportional to $e^{i(\gamma_r + i\gamma_i)z} = e^{i\gamma_r z}\, e^{-\gamma_i z}$. Thus the solution amplitude would either reduce ($\gamma_i > 0$) or grow indefinitely ($\gamma_i < 0$) with z according to the sign of γ_i. The wavelength of the reducing (or growing) fluxuations is still given by $\lambda_r = 2\pi/\gamma_r$.

The case of interest in the remainder of this paper is the one for which there are freely propagating waves of constant amplitude. This situation will result when $(\gamma/k)^2 > 1$ wherein the modified Bessel functions K_0 and K_1 have real arguments and consequently equation (12b) usually results in real roots for γ. The situation $(\gamma/k)^2 > 1$ implies the acoustic wavelength $\lambda_a = 2\pi/k$ is longer than the propagating wavelength, $\lambda_r = 2\pi/\gamma_r$.

For cylindrical shells, unlike the infinite plate, the axial membrane force N_z, will also result in a radial component of motion. Consequently, the axial and radial motions for the membrane propagation or the flexural wave propagation are coupled. In fact, the same characteristic equation (12b) can be used to determine both the membrane and flexural propagating wave numbers γ_{ax}, γ_{fl}. Whether a given root, γ, corresponds to the membrane or flexural wave can be established by examining the mode shape. More specifically, the ratio of U_0/W_0 can be solved from either of the two homogenous equations (6); upon substituting the root, γ, into say the first of equations (6) yields

$$\frac{U_o}{W_o} = \frac{\nu\gamma/a}{i\left(\frac{\omega^2}{c_p^2} - \gamma^2\right)} = \frac{\nu(\gamma/k)\, e^{i\pi/2}}{\left(\left(\frac{\gamma}{k}\right)^2 - \left(\frac{k_p}{k}\right)^2\right)(ka)} \tag{15}$$

Upon subsituting the γ/k root in question into equation (15), the size of U_o relative to W_o can be established, wherein $|U_o/W_o| >> 1.0$ implied a dominant axial motion hence signifying a membrane propagating wave and $|U_o/W_o| << 1.0$ implies a dominant radial motion hence signifying a flexural propagating wave.

Limiting Cases of General Characteristic Equation

Several limiting cases of the general characteristic equation (12b) not only provide useful information by their own merit (i.e., the traveling wave characteristic equation of a plate in fluid or air; or, the case of a cylinder in air) but at the same time provide insight with regard to where (i.e., the range of (γ/k)) to search for the root. It is instructive to start with the simplest case of an infinite flat plate in vacuo and build up to the more general case of a submerged infinite cylinder.

- infinite plate in vacuo

This situation is realized by taking the limit as the fluid to structure mass ratio goes to zero, $\rho/\rho_s \to 0$, and as the non-dimensional frequency parameters $ka \to \infty$. It is noted that $ka \to \infty$ can be realized by having the radius $a \to \infty$ at a finite frequency $\omega = k/c$. Thus equation (12b) reduces to

$$\left[k_p^2 - \gamma^2\right]\left[1 - \left(\frac{\gamma}{k_{fp}}\right)^4\right] = 0 \tag{16}$$

which by inspection has the roots

$$\gamma = k_p \quad \text{and} \quad \gamma = k_{fp}$$

Substituting $\gamma = k_p$ into equations (6) shows that

$$\begin{aligned} &U_o\, i(0) + W_o \cdot (\nu k_p/\infty) = 0 \\ &U_o\, i(0) + W_o \cdot \underbrace{[h^2 k_p^4/12 - (\omega/c_p)2]}_{\neq 0} = 0 \end{aligned} \tag{17}$$

thus, $W_o = 0$ and U_o is any constant, and hence this mode corresponds to pure axial motion with no radial motion, thus indicating the $\gamma = k_p$ root is for the membrane traveling wave. Similarly, substituting $\gamma = k_{fp}$ into equations (6) yields

$$\begin{aligned} &U_o i \overbrace{[\omega^2/c_p^2 - k_{fp}^2]}^{\neq 0} + W_o \cdot (0) = 0 \\ &U_o i\, [0] + W_o \cdot [0] = 0 \end{aligned} \tag{18}$$

thus $U_o = 0$, and W_o is any constant and hence corresponds to pure flexural motion with no axial motion.

- infinite plate in fluid

This situation is similarly obtained by passing to the limit as $a \to \infty$ in equation (12b) and noting that $(K_0(x)/K_1(x)) \to 1$ as $x \to \infty$. Thus equation (12b) reduces to

$$\left[\left(\frac{k_p}{k}\right)^2 - \left(\frac{\gamma}{k}\right)^2\right]_1 \left[1 - \frac{\left(\frac{\gamma}{k}\right)^4}{\left(\frac{k_{fp}}{k}\right)^4} + \frac{\left(\frac{\rho}{\rho_s}\right)}{kh\sqrt{\left(\frac{\gamma}{k}\right)^2 - 1}}\right]_2 = 0 \tag{19}$$

where again separate membrane traveling waves and flexural traveling waves result by separately equating the $[\ ]_1$ and $[\ ]_2$ terms to zero in quation (19). Thus by inspection, as in the in vacuo plate case,

$$\frac{\gamma}{k} = \frac{k_p}{k}$$

is again a root for the membrane propagating wave and the root of

$$\left[1 - \frac{\left(\frac{\gamma}{k}\right)^4}{\left(\frac{k_{fp}}{k}\right)^4} + \frac{(\rho/\rho_s)}{kh\sqrt{\left(\frac{\gamma}{k}\right)^2 - 1}}\right]_2 = 0 \tag{19a}$$

provides the flexural wave root. It is noted that equation (19a) is algebraically equivalent to equation (7.10) of ref. 2. Upon inspecting equation (19a), it is seen that the effect of the water presence is to make the γ/k root a larger value (i.e., the flexural wavelength is smaller) than what would have been the case in the absence of external water. Thus the water has no effect on the membrane wave root, however the flexural wave root is effected and must be solved numerically with some sort of root searching scheme.

- infinite in vacuo cylindrical shell

The characteristic equation is again obtained from the general (12b) case, by passing to the limit as $(\rho/\rho_s) \to 0$, thus obtaining

$$(k_p^2 - \gamma^2)\left[\frac{1}{a^2} - k_p^2\left\{1 - \left(\frac{\gamma}{k_{fp}}\right)^4\right\}\right] + \frac{\nu^2\gamma^2}{a^2} = 0 \tag{20}$$

which corresponds to a cubic equation in the desired γ^2 root and consequently can be solved for exactly without resorting to a numerical root finder. Due to the presence of the last term in equation (20), $\gamma = k_p$ is no longer the exact root for the membrane traveling wave, however, the $(\nu\gamma/a)^2$ does not usually shift the membrane wave number root very far from the plate solution, $\gamma = k_p$ as can be seen after solving for the exact roots of equation (20). Only positive values for γ^2 obtained from the cubic solution will correspond to freely propagating waves. Although the exact membrane and flexural roots are coupled through the last term in equation (20), an approximation of the root, say for roughing out the mesh size needed, can be obtained from the approximations

obtained after dropping the normally small $(\nu\,\gamma/a)^2$ term, hence

$$\gamma \approx k_p$$

for membrane waves, and

$$\gamma \approx k_{fp}\sqrt[4]{1 - \frac{1}{(k_p a)^2}}$$

for flexural waves.

MODELING FLEXURAL AND MEMBRANE WAVES WITH NASTRAN

A simplified model is needed for the determination of the necessary number of elements per wavelength required to accurately model the membrane and/or flexural freely propagating waves in NASTRAN type elements. The procedure used here is to cut a segment (say at least one wavelength long) out of the infinitely long model. At one cut of the model (call it the starting end "A"), moments and forces existing in the freely propagating wave are applied explicitly; at the other end (call it the termination end "B"), an appropriate absorbing boundary conditions is applied (dampers that relate shell edge velocities to edge moments and forces). The boundary absorbers implicitly apply the appropriate amount of moment or force that would have been present internally at that section of the shell. In theory, it would be possible to apply explicit appropriately phased mements and forces at the termination end as well, however, this is not done for two reasons. First, there is a certain amount of phase angle drift (an amount beyond the expected termination phase of γL) that exists as the wave propagates along the axis of the shell (or plate) and it is not known a priori what the phase drift is so that the termination moments and forces can't be appropriately adjusted; the application of boundary absorbers, however, does not require any phase drift adjustment. Secondly, the implementation of the absorbers gives future insight on how to truncate finite element shells or plates in such a manner that large problems requiring premature model termination can be made.

In Vacuo Cylindrical Shell

- determination of edge loading moments and forces

The appropriate moments and forces at the starting end A can be determined from the relationsnips relating the shell motion u, w to the shell edge loads N_Z^A, Q^A, M_Z^A and are given by the shell theory relations (ref. 1)

$$M_Z^A = D\,\frac{\partial^2 w}{\partial z^2} \qquad Q^A = D\frac{\partial^3 w}{\partial z^3} \qquad N_Z^A = \frac{Eh}{(1-\nu^2)}\left(\frac{\partial u}{\partial z} + \nu\frac{w}{a}\right) \tag{21}$$

where the equation (21) moments and forces are line loads (i.e., loads per unit circumferential arc length) obeying the shell sign convention of Figure 2a. Upon substituting equations (4) into equations (21), it follows that

$$M_Z^A = -\gamma^2 D\, W_o\, e^{i(\gamma z-\omega t)} \qquad Q^A = -i\,\gamma^3 D\, W_o\, e^{i(\gamma z-\omega t)}$$
$$N_Z^A = \frac{Eh}{(1-\nu^2)}\left[i\,\gamma\, U_o\, e^{i(\gamma z-\omega t)} + \frac{\nu}{a} W_o\, e^{i(\gamma z-\omega t)}\right] \tag{22}$$

where the relation between U_o and W_o is governed by equation (15) for cylindrical shells. For plates ($a \to \infty$), U_o and W_o are independent, where for membrane waves U_o denotes the wave amplitude with $W_o = 0$ and for flexural waves W_o is the wave amplitude with $U_o = 0$.

Equations (22) are not in a form ready to use in NASTRAN CCONEAX elements for three reasons: first, NASTRAN input is not in the usual line load form as is the case with shell theory, but rather are total values wherein the line loads must be multiplied by $2\pi a$; second, the finite element type sign convention (like quantities at both ends of the member are positive in the same sense) is different from the shell theory convention (e.g., compare Figures 2a and 2b) and; third, NASTRAN has an $e^{+i\omega t}$ hardwired into the code, consequently an adjustment in the analytical solution is necessary to compensate for this point. Specifically, a wave traveling in the +z direction also can be represented with an $i(-\gamma z + \omega t)$ type argument, thus by replacing γ with $-\gamma$ and ω with $-\omega$ in the analytical solutions will accomplish the corresponding correction. Thus accounting for all three compensations and also incorporating equation (15), the NASTRAN loading for the cylindrical shell at the starting cut A, evaluated at z = 0, is given by:

$$\tilde{M}_Z^A = 2\pi a\,\gamma^2\, D\, W_o\, e^{+i\omega t}$$
$$\tilde{Q}^A = 2\pi a\,\gamma^3\, D\, W_o\, e^{+90^o i}\, e^{+i\omega t} \qquad \text{NASTRAN cut-A loading for cylinder} \tag{23}$$
$$\tilde{N}_Z^A = \frac{2\pi a\,\rho_s\,\omega^2\nu}{(a/h)}\left(\frac{W_o}{\gamma^2-k_p^2}\right)e^{+i\omega t}$$

where W_o is any suitable displacement amplitude factor that is selected by the user, and γ is the root directly from the appropriate frequency equation (sign changes in γ and ω have already been compensated for in setting up equation (23)). The $e^{+i\omega t}$ factors are of course omitted when entered data into NASTRAN since this factor is automatically accounted for internal to the program.

- determination of shell edge termination absorbers

The membrane or flexural wave incident upon the shell termination will reflect from the end unless the appropriate boundary condition is inserted to simulate the effect of having an infinitely long shell. Here the appropriate boundary absorber is developed for each of the three shell edge loads. Following the same procedure used to setup equations (23), the internal moments and forces at the termination end are given by

$$\tilde{M}_Z^B = -2\pi a\, \gamma^2\, D\, W_o\, e^{+i\omega t}\, e^{-\gamma L}$$
$$\tilde{Q}^B = -2\pi a\, \gamma^3\, D\, e^{+i90^o}\, W_o\, e^{+i\omega t}\, e^{-i\gamma L} \qquad (24)$$
$$\tilde{N}^B = \frac{-2\pi a\, h\, \rho_s\, \omega^2 e^{+i90^o}}{\gamma} U_o\, e^{+i\omega t}\, e^{-i\gamma L}$$

The equations (24) can be written in terms of velocity, by noting $\dot{u} = +i\omega u$ $\dot{w} = i\omega w$, $dw/dx = \dot{\theta} = (-i\gamma)(i\omega w)$ thus equations (24) become

$$\tilde{M}_Z^B = \frac{-2\pi a\, \gamma\, D}{\omega}(\dot{\theta}) \qquad \tilde{Q}^B = \frac{-2\pi a \gamma^3 D}{\omega}(\dot{w}) \qquad \tilde{N}^B = \frac{-2\pi a\, h\, \rho_s \omega}{\gamma}(\dot{u}) \qquad (25)$$

where the above forces are the forces on the shell edge B. Dampers attached to the end of the shell would have an internal force or moment equal and opposite to the value at the shell edge, thus the forces and moments internal to the damper are given by

$$M_d^B = C_\theta \cdot (\dot{\theta}) \qquad Q = C_Q \cdot (\dot{w}) \qquad W = C_N \cdot (\dot{u}) \qquad (26)$$

where the damper values are given by

$$C_\theta = \frac{2\pi a\, D}{c_\gamma} \qquad C_Q = \frac{2\pi a\, D\, \gamma^2}{c_\gamma} \qquad C_N = 2\pi a h\, \rho_s c_\gamma \left\{ \begin{array}{l} \text{NASTRAN} \\ \text{CCONEAX} \\ \text{DAMPERS} \end{array} \right. \qquad (27)$$

where the propagation phase velocity, c_γ, is defined by

$$c_\gamma = \frac{\omega}{\gamma} \qquad (28)$$

where γ is the root of the characteristic equation. In the case of a plate, the same dampers can be used, except the $2\pi a$ would be replaced by the width of the plate (perpendicular to the direction of propagation) and appropriately subdivided between the element termination nodes (two termination nodes for actual plate elements and one termination node for beam elements with a plane strain correction on the Young's modulus).

Submerged Cylindrical Shell

- determination of edge loading moments and forces

The appropriate moments and forces employed to drive the shell edge employ the same equation (23) formulas, except that the propagating wave number root, γ must be determined from equations (12b) in this case.

- determination of shell edge termination dampers

Again equations (27) can be used, except that γ as determined from equations (27) is employed.

- determination of fluid loading on face z = 0

The appropriate fluid loading can be obtained by substituting equation (5a) into (5) (and converting into the $-i\gamma z + \omega t$ form by letting $\gamma = -\gamma$ and $\omega = -\omega$) to obtain

$$p(r,z) = \frac{-\rho W_0 \omega^2 H_0^{(1)}(r\sqrt{k^2-\gamma^2})}{\sqrt{k^2-\gamma^2}\, H_1^{(1)}(a\sqrt{k^2-\gamma^2})} e^{-i\gamma z + i\omega t} \tag{29}$$

Employing the large argument Bessel function approximations (ref. 5) of

$$H_0^{(1)}(X) \approx \sqrt{(2/(\pi X)}\, e^{i(X-\pi/4)} \qquad H_1^{(1)}(X) \approx H_0(X) e^{-\pi/2} \tag{30}$$

the equation (29) can be rewritten for, $|r\sqrt{\gamma^2 - k^2}| > 10.0$, in the form

$$p(r,z) \approx \frac{-W_0 \rho\omega^2 e^{-(r/a-1)(a\sqrt{\gamma^2-k^2}}}{\sqrt{\gamma^2-k^2}\,\sqrt{r/a}} e^{-i\gamma z} e^{+i\omega t} \tag{31}$$

where equation (31) can be used as the enforced pressure at the face z = 0.

Equation (31) can also be used to drive plate models by first making a change in variable r = x + a (where x is the outward distance measured from the middle surface of the shell) and then appropriately passing to the limit as $a \to \infty$ to obtain

$$p(x,z) = \frac{-W_0 \rho\omega^2 e^{-x\sqrt{\gamma^2-k^2}}}{\sqrt{\gamma^2-k^2}} e^{-i\gamma z} e^{+i\omega t} \tag{32}$$

- decermination of fluid loading on face z = L

On this face we choose to absorb the incident pressure wave with an absorber type boundary condition rather than load it explicitly with equation (29) evaluated at z = L. This approach is consistent with the manner in which the shell was terminated. The relationship between pressure and applied forces in a finite element formulation is that the normal gradient of the pressure is proportional to the finite element model force. Therefore, the gradient of pressure normal to the cut, z = L is needed and given by (with equation (5)$i(+\gamma z - \omega t)$ arguments)

$$\frac{\partial p}{\partial z} = i\gamma p(r,z) \tag{34}$$

and since for steady state problems,

$$\frac{\partial p}{\partial t} = -i\omega p$$

it follows

$$\frac{\partial p}{\partial z} = \frac{-\gamma}{\omega}\frac{\partial p}{\partial t} \equiv \frac{-\gamma}{\omega}\dot{p} \tag{35}$$

is the boundary condition to employ along the vertical fluid cut z = L. For direct acoustic fluid elements (ref. 6), the finite element nodal force is related to the normal gradient by the relation

$$F_n = \int_S [N]^T \frac{\partial p}{\partial n'} \, dS \tag{36}$$

where [N] is the element shape function. For lumped force applications, equation (36) is represented as, (where n' is the unit normal to the fluid and ΔA is an appropriate amount of area surrounding the node at the point of the F_n application)

$$F_n = \Delta A \frac{\partial p}{\partial n'} \tag{37}$$

and upon substituting equation (35) intc (37) one obtains

$$F_n = -\Delta A \frac{\gamma}{\omega} \dot{p} \tag{38}$$

and represents the nodal force on the fluid as being proportional to the pressure time rate of change. Thus the internal force in a damper attached to the node would be equal and opposite in value and given by

$$F_n^{damp} = +\Delta A \frac{\gamma}{\omega} \dot{p}$$

where the damper value would be

$$C_d^p = \frac{\Delta A \gamma}{\omega} \qquad \begin{array}{l}\text{direct pressure method damper} \\ \text{(no analogy) for z = L face}\end{array} \tag{39}$$

In the case of NASTRAN, the acoustic fluid is modeled by way of an analogy which reduces the elasticity equations to the Helmholtz equation by way of introducing dummy constants into the material matrix and allowing the displacement variable, u_z, occupy the pressure variable (see ref. 3 for details). The analogy has been adopted herein, consequently, an additional factor of ρc^2 appears in equation (37), and consequently the frequency dependent NASTRAN axial damper needs to be modified by this same factor and thusly equation (39) is replaced by (replacing $\omega \to -\omega$, $\gamma \to -\gamma$ converts to NASTRAN convention; this results in the same damper since signs cancel)

$$\tilde{C}_d^p = \frac{\Delta A \gamma}{\omega} \rho c^2 \qquad \begin{array}{l}\text{NASTRAN (ref. 3) analogy damper} \\ \text{for z = L face, with } \gamma \text{ directly from} \\ \text{appropriate characteristic equation.}\end{array} \tag{40}$$

It is noted, that so long as γ is a real quantity (e.g., characteristic root equation for γ is obtained from equation (12b)), the termination condition in the z direction is a pure damper. However, where γ is complex (e.g., root from equation (12a)) substitution of γ into the equation (40) damper will result in a complex damper. The real part can be treated as above, but the complex part will end up looking like a resistance (spring) when combined with the $+i\omega$ appearing as a multiplier in the assembled damping matrix in NASTRAN. Thus, the imaginary part of the damper (if it is present) can be applied as a nodal spring whose spring constant is

$$\left(\frac{i\Delta A(-\gamma^i)}{(-\omega)} \rho c^2\right)(+i\omega) = -\Delta A \, \rho c^2 \, \gamma^i \qquad \begin{array}{l}\text{NASTRAN analogy spring} \\ \text{(with } \gamma^i \text{ directly from} \\ \text{appropriate characteristic} \\ \text{equation)}\end{array}$$

wherein for decaying waves, γ^i will be a positive number making the spring constant positive.

Equation (40) can equally be applied to plate model problems, upon properly interpreting ΔA.

- determination of fluid loading on outer face $r = r_o$

Here on the outer radial fluid face, the boundary condition is developed just as in the previous case, except that now the gradient has to be taken in the direction of the outward normal ($n' = r$). Thus operating on equation (29) with $\partial(\ )/\partial r$ and then employing the equation (30) large argument relations, the following result is obtained

$$\frac{\partial p}{\partial r} \approx -\sqrt{\gamma^2 - k^2}\, p(r,z) \tag{41}$$

Unlike equation (34), this result does not have a factor i relating the gradient of p and p itself, consequently, upon substition of equation (41) into equation (37), one obtains

$$F_n = -\Delta A \sqrt{\gamma^2 - k^2}\; p \tag{42}$$

and represents the nodal force on the fluid as being proportional to the pressure. Thus the internal force in a spring attached to the node would be equal and opposite in value and is given by

$$F_n^{spg} = +\Delta A \sqrt{\gamma^2 - k^2}\; p$$

where the spring constant value would be

$$K^p = \Delta A \sqrt{\gamma^2 - k^2} \qquad \begin{array}{l}\text{direct pressure method spring} \\ \text{(no analogy) for } r = r_o \text{ face}\end{array} \tag{43}$$

and in the case of employing the ref. 3 pressure analogy, the counterpart of equation (43) is

$$\tilde{K}^p = \Delta A\, \rho c^2 \sqrt{\gamma^2 - k^2} \qquad \begin{array}{l}\text{NASTRAN (ref. 3) analogy} \\ \text{spring for } r = r_o \text{ face}\end{array} \tag{44}$$

When γ is a root of equation (12b) ($\gamma^2 > k^2$), equation (44) implies a real spring is all that is needed. However, when $\gamma^2 < k^2$, and equation (12a) is employed, the roots, γ, are, in general, complex which implies that equation (44) will have a real and imaginary part. The real part of $\tilde{K}^p$ is still a spring, however the imaginary portion can be converted into a damper by dividing the imaginary part coefficient (not including i) of equation (44) by ω (to compensate for the ω multiplied in by the complex stiffness formation).

Equation (44) can equally be applied to plate model problems, upon appropriately interpreting ΔA.

Limitations of Membrane and Flexural Wave Modeling

The scope of this study is limited to a driving frequency region where the influence of plate rotary inertia and shear deformation on the flexural motions are not important. In fact, this is the limitation of the propagating wavelength formulas given earlier. The ability of NASTRAN to account for these higher order effects is a topic all in itself and will not be addressed in this paper wherein stiffness and mass formulations along the lines given in ref. 7 must be considered.

Although we are interested in both plate and shell propagating waves, the classical plate theory (CPT) can provide insight with regard to the point at which theabove mentioned correction factors are needed. The CPT is defined here as the special case of equation (1) with $a \to \infty$. Midlin's classical paper (ref. 4) provides a guideline for when the characteristic wave equations presented herein no longer predicts the proper waves number roots, γ. As pointed out in ref. 4, the exact elasticity solution to the same problem shows that CPT can predict the correct flexural wave numbers when the corresponding $2\pi/\gamma$ wavelengths are long in comparison with the thickness of the plate. As the wavelength gets smaller, the exact elasticity solution traveling wave phase velocity (ω/γ), has as its upper limit, the velocity of the Rayleigh surface wave. Hence the CPT cannot be expected to give good results for the wave numbers, γ, as the driving frequencies get increasingly large. Reference 4 provides a plot of propagating phase velocity $c_\gamma = \omega/\gamma$ (non-dimensionalized with respect to the shear wave velocity $c_s = \sqrt{G/\rho_s}$) versus the plate thickness (non-dimensionalized with respect to the flexural wavelength, $2\pi/\gamma$ for a fixed Poisson's ratio ($\nu = 0.5$) and is reproduced here as Figure 3. The CPT straight line plot, curve II, is nothing more than equation (9) rewritten in the form

$$\frac{c_\gamma}{c_s} = \frac{h}{\lambda_\gamma} \cdot \frac{2\pi}{\sqrt{6(1-\nu)}} \tag{44a}$$

and is compared against curve I, the exact elasticity solution. Curves III, IV, and V are different combinations of adding rotary interior and shear correction factors. Figure 3 suggests that the shear correction addition has the biggest impact on correcting the CPT case. The shear thickness parameter T2, in the NASTRAN CCONEAX elements appears to attempt to account for shear effects, however, this point has not been pursued with regard to attempting to make NASTRAN propagate flexural waves for $h/\lambda_\gamma > 0.15$.

The results in Figure 3 suggest that a h/λ_γ (plate thickness-to-flexural wavelength ratio) of limit of 0.15 be maintained, i.e.,

$$\frac{h}{\lambda_\gamma} \leq 0.15 \tag{45}$$

or equivalently,

$$\frac{\gamma h}{2\pi} \leq 0.15 \tag{45a}$$

where γ is the flexural wave number root of the problem at hand. The limit given by equation (45a) employed Figure 3 which is a plot based on a fixed Poisson's ratio (i.e., $\nu = 0.5$). The guideline formula can still be used for other values of Poisson's ratio due to the weak dependence of the plots on ν. In fact, for the common case of $\nu = 0.3$, a value of $h/\lambda_\gamma = 0.15$ implies a c_γ/c_s ordinate of 0.4598 for the CPT case and a value of 0.4032 in the exact

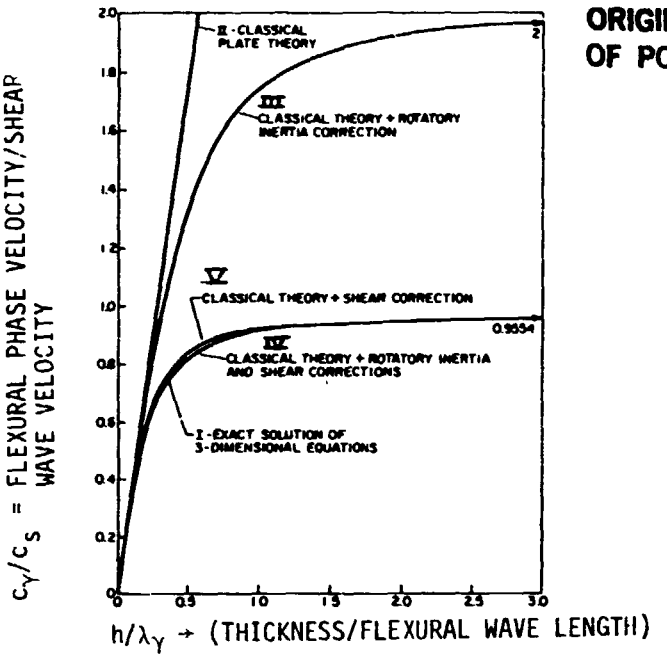

FIGURE 3. DEVIATION OF THIN WALL PLATE THEORY FROM EXACT THEORY

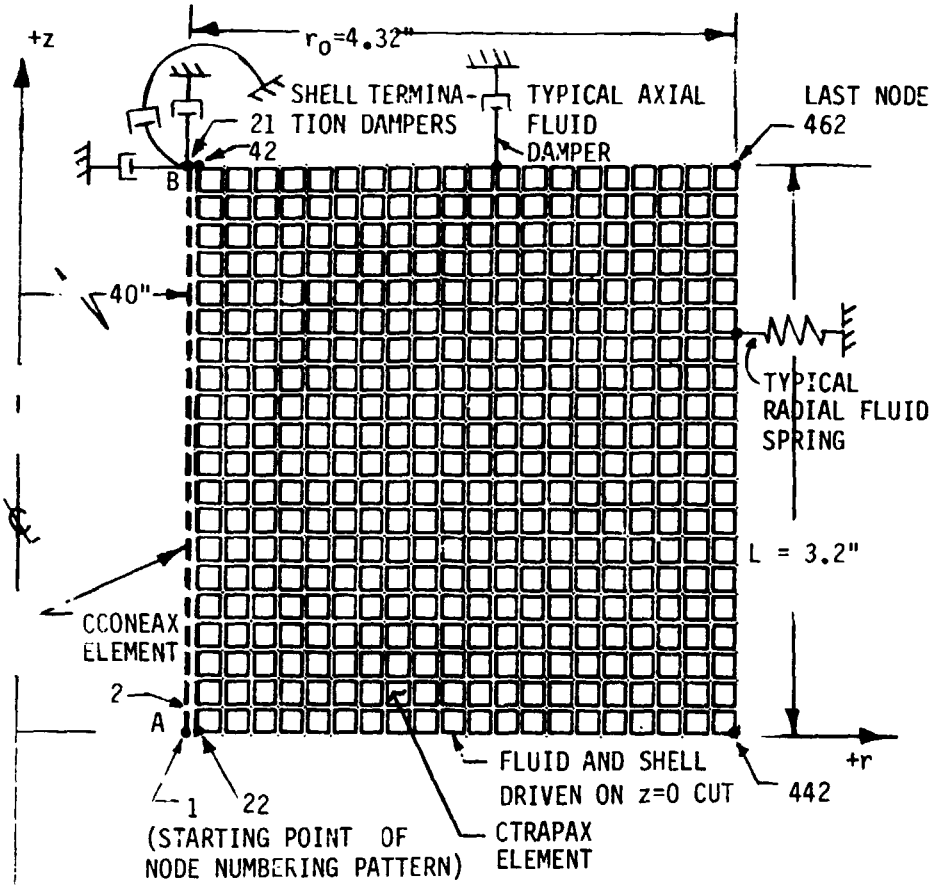

FIGURE 4. FINITE ELEMENT MESH (20-ELEMENT SHELL)

theory case. However, for $\nu = 0.5$, a $h/\lambda_\gamma = 0.15$ implies a c_γ/c_s ordinate of 0.5441 in the CPT case and a value of 0.4629 in the exact theory case (computed from equation (40) of ref. 4). Thus, illustrating the Figure 3 $\nu = 0.5$ case is an extreme case (e.g., 17.5% deviaton for $\nu = 0.5$ compared to 14.0% for $\nu = 0.3$) with regard to the point at which CPT deviates from the exact theory.

Thus, to test inequality (45a), one simply employs the appropriate characteristic equation developed (e.g., equation (12b)) and after obtaining the flexural wave root γ, verify whether in equation (45a) is satisfied.

Comments on Mass Matrix

The issue of an appropriate mass matrix for dynamics problems has long been a topic of discussion in the literature on finite elements. Here we take the simpliest approach, namely that of a diagonal lumped mass matrix for the shell. Upon employing the lumped approach, for say CCONAX elements, NASTRAN generates zero valued rotary inertia mass matrix contributions. To fill this void, the work by ref. 8 was employed wherein the suggested diagonal rotary inertia terms at a node would be given by

$$I_r = \frac{m^e \ell^2}{24}\left[\frac{1}{10} + \left(\frac{h}{\ell}\right)^2\right] \tag{46}$$

for the single element contribution at a rotation degree-of-freedom node where m^e is the total mass of the element, ℓ is the element length, h the element thickness. Thus end point nodes with one element framing into the node employs equation (46) once and internal nodes with two elements framing into the same node applys equation (46) twice.

DEMONSTRATION PROBLEMS

A series of limited, yet fully representative, demonstration problems are presented here to illustrate the use of the procedures discussed in the theoretical section. First an in vacuo cylindrical shell is treated employing three different mesh distributions. Secondly, the same shell (employing the finer mesh distribution) is solved with external water present. All solutions are obtained with COSMIC SOL-8 employing the VAX computer version of NASTRAN.

In Vacuo Cylinder Example

An infinite cylindrical shell is excited and is propagating a constant amplitude harmonic wave in the plus z direction. The shell (shown in Figure 1) is cut at points A and B and is modeled as a 3.2 inch long, 20 element CCONEAX finite element model shown in Figure 4 (in the in vacuo case considered here, the fluid is omitted in the model). The point A (incident side of the shell) is driven with equations (23) and is terminated with three boundary dampers sized according to equations (27). The problem parameters correspond to the following data

$$a = 40.0" \quad , \quad h = 0.20" \quad , \quad E = 154{,}149.39 \text{ psi}$$
$$\nu = 0.3 \quad , \quad \rho_s = 0.000048, \quad \omega = 9749.99 \text{ rad/sec} \tag{47}$$

wherein the corresponding wave number roots to the characteristic equation (20) are given by

$$\gamma = 0.163949685 \quad \text{for the membrane root}$$
and
$$\gamma = 1.67707302 \quad \text{for the flexural wave root} \tag{48}$$

hence the membrane wavelength is 12.566 inches and the flexural wavelength is 3.7465 inches.

- flexural wave example

The shell termination dampers at cut B are computed upon substitution of the equation (48) flexural wave root into equations (27) to obtain

$$C_\theta = 4.8819909 \qquad C_Q = 13.7309605 \qquad C_N = 14.0269417 \tag{49}$$

and the shell edge forces, for an arbitrarily selected driven amplitude of $W_o = 1.0 \times 10^{-6}$, at the driver cut end A are obtained by substituting the flexural wave root into equations (23) to obtain (supressing the exponential time factor where dampers are installed with DMIG cards):

$$\tilde{M}_Z^A = 7.9827681 \times 10\text{-}2 \qquad \tilde{Q}^A = 0.1338768\ e^{i\pi/2}$$
$$\tilde{N}_Z^A = 6.175285 \times 10\text{-}4 \tag{50}$$

The rotary inertia mass entries are computed with equation (46). The corresponding NASTRAN input is given in Figure 5 for reference purposes. The exact solution is a constant amplitude displacement wave varying as

$$w = W_o\ e^{i(-\gamma z + \omega t)}$$

Consequently, the exact solution is easy to plot and is simply a constant magnitude radial displacement of magnitude $W_o = 1 \times 10\text{-}6$ and whose phase angle rolls off linearly with z and reploting with spatial period $2\pi/\gamma$. The exact solution versus the NASTRAN solution is given in Figure 6 and shows good agreement between the exact solution and the corresponding NASTRAN solution. Since the model element spacing is 0.16 inches, the solution model is a 23½ element per wavelength case. In order to investigate the influence of mesh size on solution accuracy, the same 3.2 inch model was run for two coarser meshes; one having 5 elements and the other having only 3 elements. The same dampers and edge loads are reapplied to the coarser models. The resulting solutions are shown in Figure 7 and as can be seen, the quality of the solution (i.e., the ability of the cylindrical shell to propagate flexural waves) has degraded over the finer mesh example, particularly for the three element shell.

```
ID NUSC, FLEX WAVE IN SHELL WITH FORCE LOADING
DIAG 8,14
APP DISP
SOL 8
TIME 2400
CEND
TITLE= FLEX WAVE IN SHELL WITH FORCE LOADING
R2PP=DASH
M2PP=MASS
AXISYMMETRIC=COSINE
SDISPLACEMENTS(PHASE)=ALL
FREQUENCY=100
MAXLINES=600000
DLOAD=ALL
DLOAD=100
BEGIN BULK
AXIC           0
FREQ         100 1551.76
MAT1         600154149.6                .3 .000048
PCONFAX      160      600      .20      600.0006667      600      .167      0.0+PCON
+PCON          1.       -1.       0.       90.      180.
RLOAD2       400      101                103     1000
TABLED1     1000                                                          +TAB1
+TAB1          1.0      1.0  10000.       1.0     ENDT
DLOAD        100       1.       1.       400       1.      401
RLOAD2       401      889                        1000
DAREA*                889                1000001                5      7.9827681-2
DPHASE       103 1000001                1     90.
DAREA*                101                1000001                1        .1338768
DAREA*                889                1000001                3      6.175285-4
DMIG    DASH     0        1          1         1
DMIG*                 DASH             1000021                1                    *DASH1
*DASH1              1000021                    1      13.7309605
DMIG*                 DASH             1000021                3                    *DASH3
*DASH3              1000021                    3      14.0269417
DMIG*                 DASH             1000021                5                    *DASH2
*DASH2              1000021                    5       4.8819909
DMIG    MASS     0        1          1         1
DMIG         MASS 1000001        5           1000001        5 6.988-7
DMIG         MASS 1000002        5           1000002        5 1.397-6
DMIG         MASS 1000003        5           1000003        5 1.397-6
DMIG         MASS 1000004        5           1000004        5 1.397-6
DMIG         MASS 1000005        5           1000005        5 1.397-6
DMIG         MASS 1000006        5           1000006        5 1.397-6
DMIG         MASS 1000007        5           1000007        5 1.397-6
DMIG         MASS 1000008        5           1000008        5 1.397-6
DMIG         MASS 1000009        5           1000009        5 1.397-6
DMIG         MASS 1000010        5           1000010        5 1.397-6
DMIG         MASS 1000011        5           1000011        5 1.397-6
DMIG         MASS 1000012        5           1000012        5 1.397-6
DMIG         MASS 1000013        5           1000013        5 1.397-6
DMIG         MASS 1000014        5           1000014        5 1.397-6
DMIG         MASS 1000015        5           1000015        5 1.397-6
DMIG         MASS 1000016        5           1000016        5 1.397-6
DMIG         MASS 1000017        5           1000017        5 1.397-6
DMIG         MASS 1000018        5           1000018        5 1.397-6
DMIG         MASS 1000019        5           1000019        5 1.397-6
DMIG         MASS 1000020        5           1000020        5 1.397-6
DMIG         MASS 1000021        5           1000021        5 6.988-7
RINGAX         1                      40.00     0.00                          246
RINGAX         2                      40.00     0.16                          246
RINGAX         3                      40.00     0.32                          246
RINGAX         4                      40.00     0.48                          246
RINGAX         5                      40.00     0.64                          246
RINGAX         6                      40.00     0.80                          246
RINGAX         7                      40.00     0.96                          246
RINGAX         8                      40.00     1.12                          246
RINGAX         9                      40.00     1.28                          246
RINGAX        10                      40.00     1.44                          246
RINGAX        11                      40.00     1.60                          246
RINGAX        12                      40.00     1.76                          246
RINGAX        13                      40.00     1.92                          246
RINGAX        14                      40.00     2.08                          246
RINGAX        15                      40.00     2.24                          246
RINGAX        16                      40.00     2.40                          246
RINGAX        17                      40.00     2.56                          246
RINGAX        18                      40.00     2.72                          246
RINGAX        19                      40.00     2.88                          246
RINGAX        20                      40.00     3.04                          246
RINGAX        21                      40.00     3.20                          246
CCONEAX        1        160          1         2
CCONEAX        2        160          2         3
CCONEAX        3        160          3         4
CCONEAX        4        160          4         5
CCONEAX        5        160          5         6
CCONEAX        6        160          6         7
CCONEAX        7        160          7         8
CCONEAX        8        160          8         9
CCONEAX        9        160          9        10
CCONEAX       10        160         10        11
CCONEAX       11        160         11        12
CCONEAX       12        160         12        13
CCONEAX       13        160         13        14
CCONEAX       14        160         14        15
CCONEAX       15        160         15        16
CCONEAX       16        160         16        17
CCONEAX       17        160         17        18
CCONEAX       18        160         18        19
CCONEAX       19        160         19        20
CCONEAX       20        160         20        21
ENDDATA
```

FIGURE 5. TWENTY ELEMENT CYLINDRICAL SHELL EXAMPLE DATA FOR FLEXURAL WAVE RUN

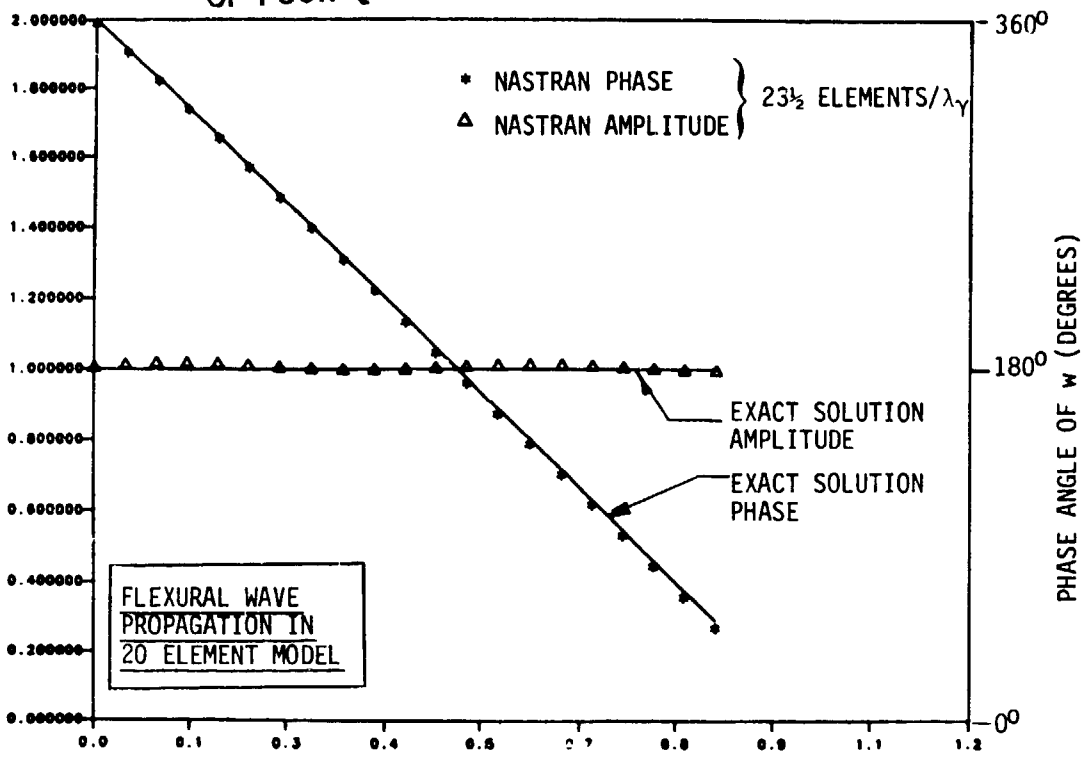

FIGURE 6. RADIAL SHELL DISPLACEMENT VS. AXIAL COORDINATE (FINE MESH) FOR 23½ FLEXURAL WAVE LENGTHS PER ELEMENT

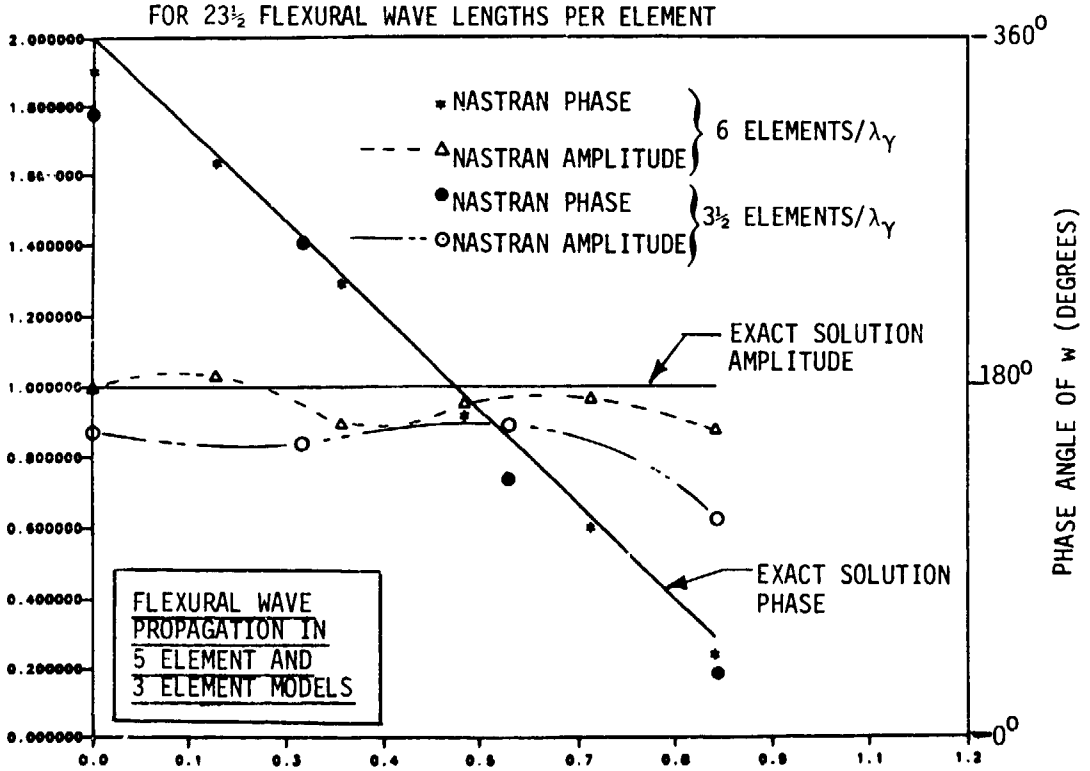

FIGURE 7. RADIAL SHELL DISPLACEMENT VS. AXIAL COORDINATE (COARSE MESH) FOR 6 AND FOR 3½ FLEXURAL WAVE LENGTHS PER ELEMENT

- membrane wave example

Again, the 20 element model is considered, except in this case, we propagate a membrane wave along the +z direction of the same cylindrical shell considered for the flexural wave example. The procedure is exactly the same here, except that the membrane root (first of equations (48)) is employed to compute the shell termination dampers and driving moments and forces. Thus, substituting the membrane root into equations (27) and (23), the model dampers and edge loads are in this case:

$$C_\theta = 0.4772607 \qquad C_Q = 0.012828529 \qquad C_N = 143.484479$$

and

$$\tilde{M}_Z^A = 7.6290549 \times 10\text{-}4 \qquad \tilde{Q}^A = 1.2507811 \times 10\text{-}4\ e^{i\pi/2}$$

$$\tilde{N}_Z^A = -29.909871$$

The solution response for the dominant axial motion is plotted in Figure 8 and is non-dimensionalized with respect to the, U_o, axial wave amplitude magnitude (by equation (15), $|U_o| = 21.37985 \times 10\text{-}6$ when $W_o = 1.0 \times 10\text{-}6$). The radial deflection, non-dimensionalized with respect to W_o, is given in Figure 9. The quality of the solution is seen to be very accurate, as would be expected since the wavelength is substantially longer than the flexural wave example (e.g., $(2\pi/.0163949)/0.16 = 239\frac{1}{2}$ elements per wavelength.

Submerged Cylinder Example (Flexural Wave)

Again, the same 20 element cylindrical shell is considered, except here, the shell is submerged in water (external water only where c = 60,000. in/sec and $\rho = 0.000096$). Substituting the equation (47) parameters into equation (7b), and solving for the wave number roots, it is found that

$$\gamma = 0.164124528 \qquad \text{for the membrane root}$$

and (51)

$$\gamma = 2.51631787 \qquad \text{for the flexural root.}$$

Comparing the second of equations (51) to the in vacuo wave number, it is noted that the presence of the fluid shortened the wavelength by a factor of$\approx 2/3$. Substituting the flexural root into equations (27) and (23), the model dampers and edge loads (for a $W_o = 1 \times 10\text{-}6$ shell amplitude) are given by

$$C_\theta = 7.32505101 \quad , \quad C_Q = 46.3811654 \quad , \quad C_N = 9.34867391$$

and

$$\tilde{M}_Z^A = 0.179713448 \quad , \quad \tilde{Q}_A = 0.452216160\ e^{i\pi/2} \quad ,$$

$$\tilde{N}_Z^A = 2.7283602 \times 10\text{-}4$$

In addition, the z = L boundary cut damper is given through equation (40), the $r = r_Q = 43.2$ inch fluid boundary spring by equation (44) and the z = 0 pressure loading by equation (31). The pressure values are enforced by applying the stiff spring approach, where the stiff spring constant is sized to be 1000

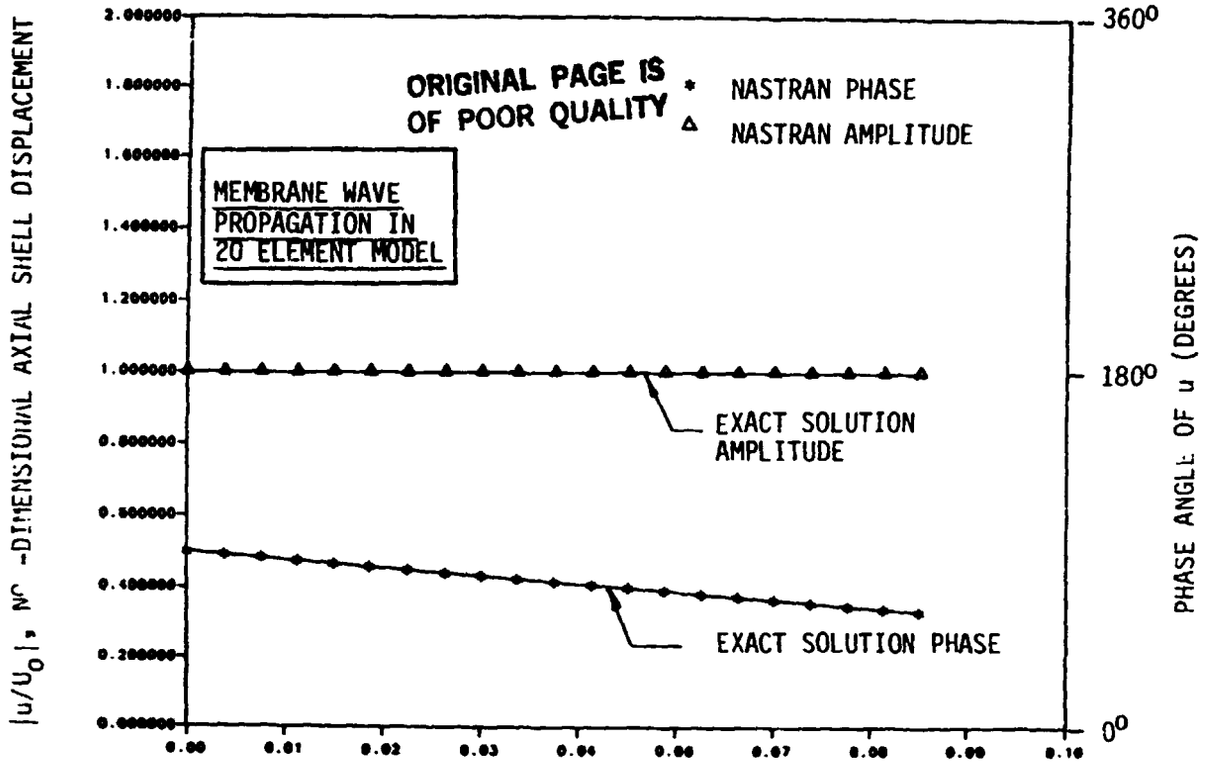

FIGURE 8. AXIAL SHELL DISPLACEMENT VS. AXIAL COORDINATE (FINE MESH)

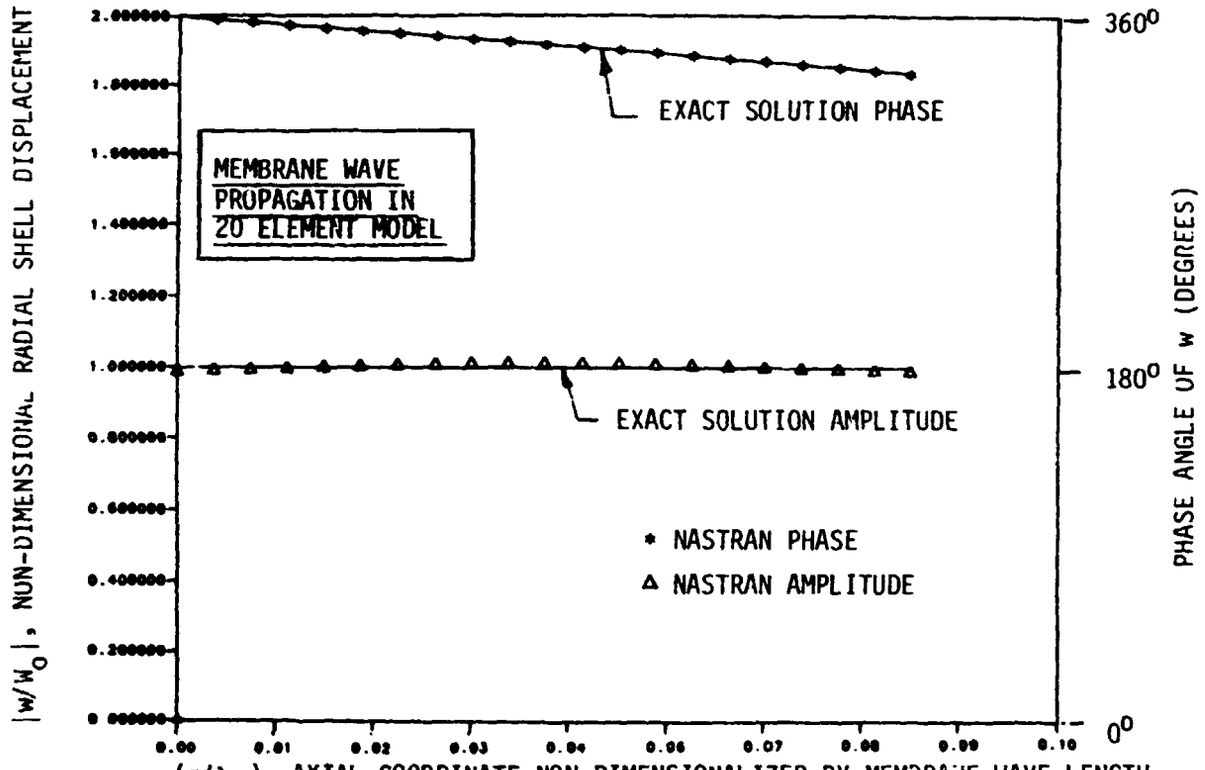

FIGURE 9. RADIAL SHELL DISPLACEMENT VS. AXIAL COORDINATE (FINE MESH)

times the regular pressure element stiffnesses and the applied force is the pressure times the stiff spring. The actual data input is shown in Figure 10, where the obvious repetitive pattern to the numbering system of Figure 4, permits us to leave out most of the grid coordinate cards, element cards, and fluid-to-structure DMIG connection cards while leaving behind representative examples of each kind. The resulting response for the radial deflection is plotted in Figure 11 and the corresponding pressure in the fluid (at the surface of the structure) is plotted in Figure 12. Both the deformation and pressure are seen to track the exact solution closely. A graphical representation of the entire pressure field amplitude is shown in Figure 13 through employing the PATRAN fringe color plotting feature. Plotting data in this fashion shows bands of data having the same magnitude spread, as a single color. Narrow bands at the surface spreading outward radially to increasingly wider bands show the exponential type decay in the pressure field.

CONCLUDING REMARKS

The results in this paper demonstrate a procedure by which the NASTRAN computer program can be employed to check the ability of the NASTRAN program to model membrane and flexural waves existing in both in vacuo and submerged cylindrical shells and flat plates. The study is limited to a range of frequencies where rotary inertia and shear correction factors are not necessary to model the corresponding wave propagation. For the demonstration problems considered, the wave propagation ability of the elements considered appears to fall off rapidly, once lessthan 6 elements per wavelength are considered. For example, in the 6 element per flexural wavelength problem, the worse nodal point magnitude was in error by 12 % for the radial deflection, whereas the error was 36.7% for the 3½ element per wavelength example. It is recommended that the user make his own test with regard to mesh fineness necessary to achieve a particular level of accuracy. For example, when the propagating wave root is in the neighborhood of a cutoff frequency (i.e., a condition where no propagating wave exists), finer meshes than experineced in the demonstration considered in this paper may be needed. For most cases experienced by the authors, however, 10 elements per wavelength appears to provide good results for properly modeling the wave propagation for flexure and membrane waves in the kinds of elements considered herein.

```
TO NUSC, FLEX WAVE WITH WATER LOADING
DIAG 8,14
APP DISP
SOL 8
TIME 2400
CEND
TITLE= FLEX WAVE WITH WATER LOADING FREQUENCY=15517.61 HZ
B2PP=DASH
M2PP=MASS
K2PP=STIF
AXISYMMETRIC=COSINE
SDISPLACEMENTS(PHASE)=ALL
FREQUENCY=100
MAXLINES=600000
OLOAD=ALL
DLOAD=100
BEGIN BULK
AXIC            0
FREQ          100 1551.76
MAT1          600154149.6               .3 .000048
PCONEAX       160     600     .20    600.0006667     600    1.67    0.0+PCON
+PCON          1.     -1.      0.      90.    180.
PLOAD2        400     104                     1000                          +TAB1
TABLED1      1000
+TAB1         1.0     1.0  10000.      1.0    ENDT
DLOAD         100      1.      1.      400      1.     402
PTRAPAX       150              500
MAT1          500          345600.  50000. .000096
PLOAD2        402     888              103    1000
DAREA         104 1000001       5.1797134
DPHASE        103 1000001       1      90.
DAREA         888 1000001       1.4522162
DAREA         104 1000001       32.7284-4
DMIG         DASH 1000021       1             1000021        146.38117
DMIG         DASH 1000021       3             1000021        39.348674
DMIG         DASH 1000021       5             1000021        57.325051
DMIG     STIF   0       1       1       1
DMIG     MASS   0       1       1       1
DMIG     DASH   0       1       1       1
DAREA*                  104             1000022                 3       -.363431E+11
DAREA*                  104             1000043                 3       -.242700E+11
DAREA*                  104             1000064                 3       -.162076E+11
DAREA*                  104             1000085                 3       -.108236E+11
DAREA*                  ...             1000106                 .       -.7229...
.AREA*          :                       100..           :
D..                                     10..
*   1.5                 1000358                 3                               *
DMIG*    STIF                           1000379
*   185                 1000379                 3                 1.E+13
DMIG*    STIF                           1000400                        3        *   195
*   195                 1000400                 3                 1.E+13
DMIG*    STIF                           1000421                        3        *   205
*   205                 1000421                 3                 1.E+13
DMIG*    STIF                           1000442                        3        *   215
*   215                 1000442                 3                 1.E+13
DMIG*    STIF                           1000443                        3        *   A25
*   A25                 1000443                 3 37689064.000000
DMIG*    STIF                           1000444                        3        *   A35
*   A35                 1000444                 3 37689064.000000
DMIG*    STIF                           1000445                        3        *   A45
*   A45                 1000445                 3 37689064.000000
.MIG*    STIF                           ..0446                         3        .   .55
*   .55                 1000.                     ..89068.000000
*                       :                                       :
DMIG*                                   1000461                                 *   .2..
*   A205                ..00461                 3 3768900 .
DMIG*    STIF                           1000462                        3        *   A215
*   A215                1000462                 3 18844542.000000
DMIG*    DASH                           1000462                        3        *   AB15
*   AB15                1000462                 3     1933.227905
DMIG*    DASH                           1000441                        3        *   AB25
*   AB25                1000441                 3     3859.287471
DMIG*    DASH                           1000420                        3        *   AB35
*   AB35                1000420                 3     3844.935547
.MIG*    DASH                           1000399                        3        *   AB45
                        :                       3               :
.                                       ..00...
*   AB205               ....003                 3     30.. .
DMIG*    DASH                           1000042                        3        *   AB2..
*   AB215               1000042                 3     1796.933472
DMIG*    STIF                           1000022                        3        *    10
*    10                 1000001                 1       20.106194
DMIG*    STIF                           1000022                        3        *    11
*    11                 1000001                 3        0.000001
DMIG*    MASS                           1000001                        1        *    12
*    12                 1000022                 3     -667.075256
DMIG*    MASS                           1000001                        3        *    13
*    13                 10000..                 3       -0.000029
.        STIF.          ..016       .           ...
DMIG         :  . 1000017       5                      :        . 1.397-6
DMIG         MASS 1000018       5                1000018        5 1.397-6
DMIG         MASS 1000019       5                1000019        5 1.397-6
DMIG         MASS 1000020       5                1000020        5 1.397-6
DMIG         MASS 1000021       5                1000021        5 6.984-7
RINGAX          1               40.00   0.00                          246
RINGAX          2               40.00   0.16                          246
RINGAX          3               40.00   0.32                          246
RINGAX          4               40.00   0.48                          246
RINGAX          5               40.00   0.64                          246
                6                       . .80                         246
RI
RINGAX          :               43.20   ....                        12456
RINGAX        460               43.20   2.86                        12456
RINGAX        461               43.20   3.04                        12456
RINGAX        462               43.20   3.20                        12456
CCONEAX         1     160       1       2
CCONEAX         2     160       2       3
CCONEAX         3     160       3       4
CCONEAX         4     160       4       5
..ONEAX         5     160       5       .
.               6     160               ..
CCON...         :               18      19
CCONEAX        19     160      19      20
CCONEAX        20     160      20      21
CTRAPAX        21     150      22      43      44      23
CTRAPAX        22     150      23      44      45      24
CTRAPAX        23     150      24      45      46      25
..RAPAX        24     150      25      46      47      26
               25     150      26      47      48      27
         :              .150    .       .      49      28
                                                      460      ..
CTRAPAX       419     150     ...     460     461      ..
CTRAPAX       420     150     440     461     462     441
ENDDATA
```

FIGURE 10. TWENTY ELEMENT SUBMERGED SHELL EXAMPLE DATA FOR FLEXURAL WAVE RUN

ORIGINAL PAGE IS
OF POOR QUALITY

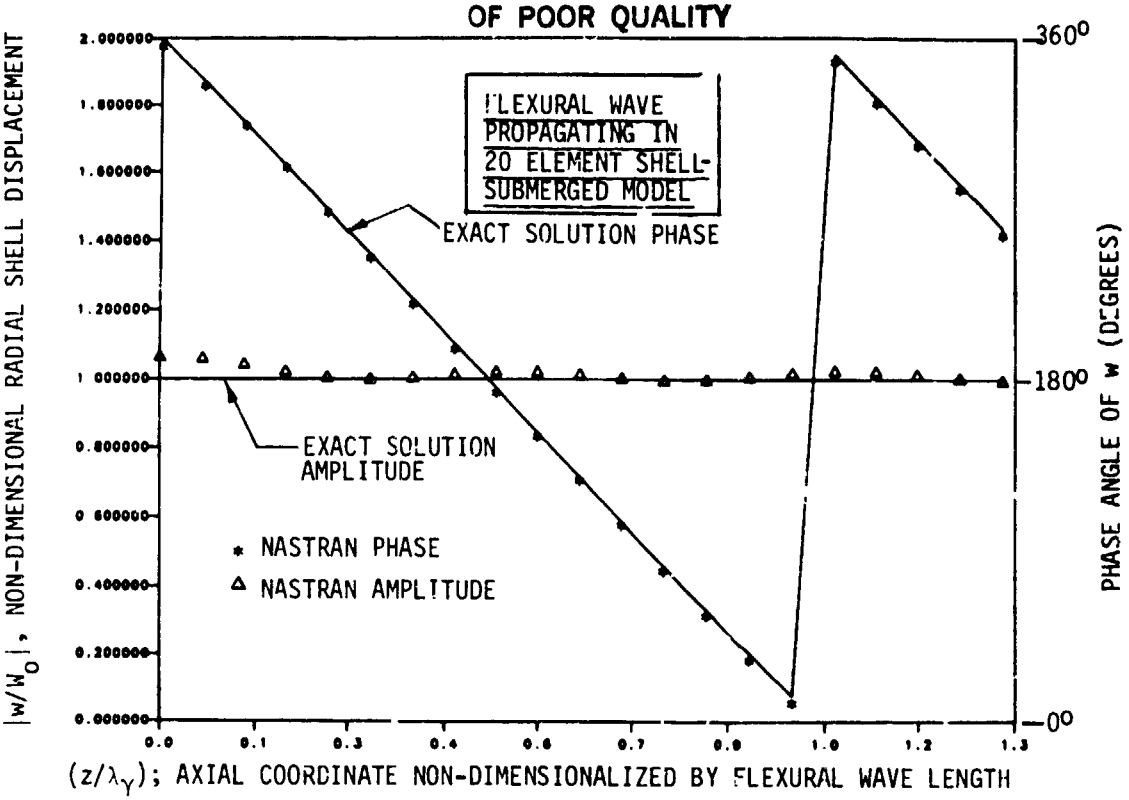

FIGURE 11. RADIAL DISPLACEMENT VS. AXIAL COORDINATE FOR 15½ FLEXURAL WAVE LENGTHS PER ELEMENT (SUBMERGED SHELL)

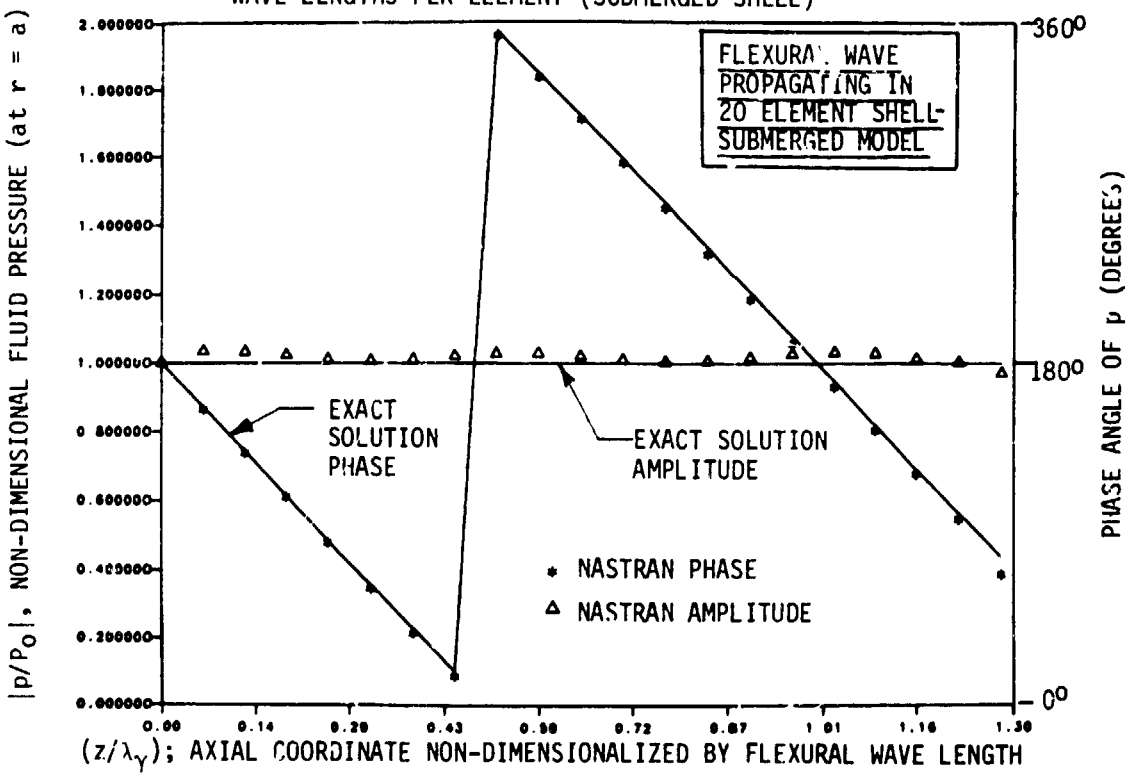

FIGURE 12. SURFACE PRESSURE VS. AXIAL COORDINATE FOR 15½ FLEXURAL WAVE LENGTHS PER ELEMENT (SUBMERGED SHELL)

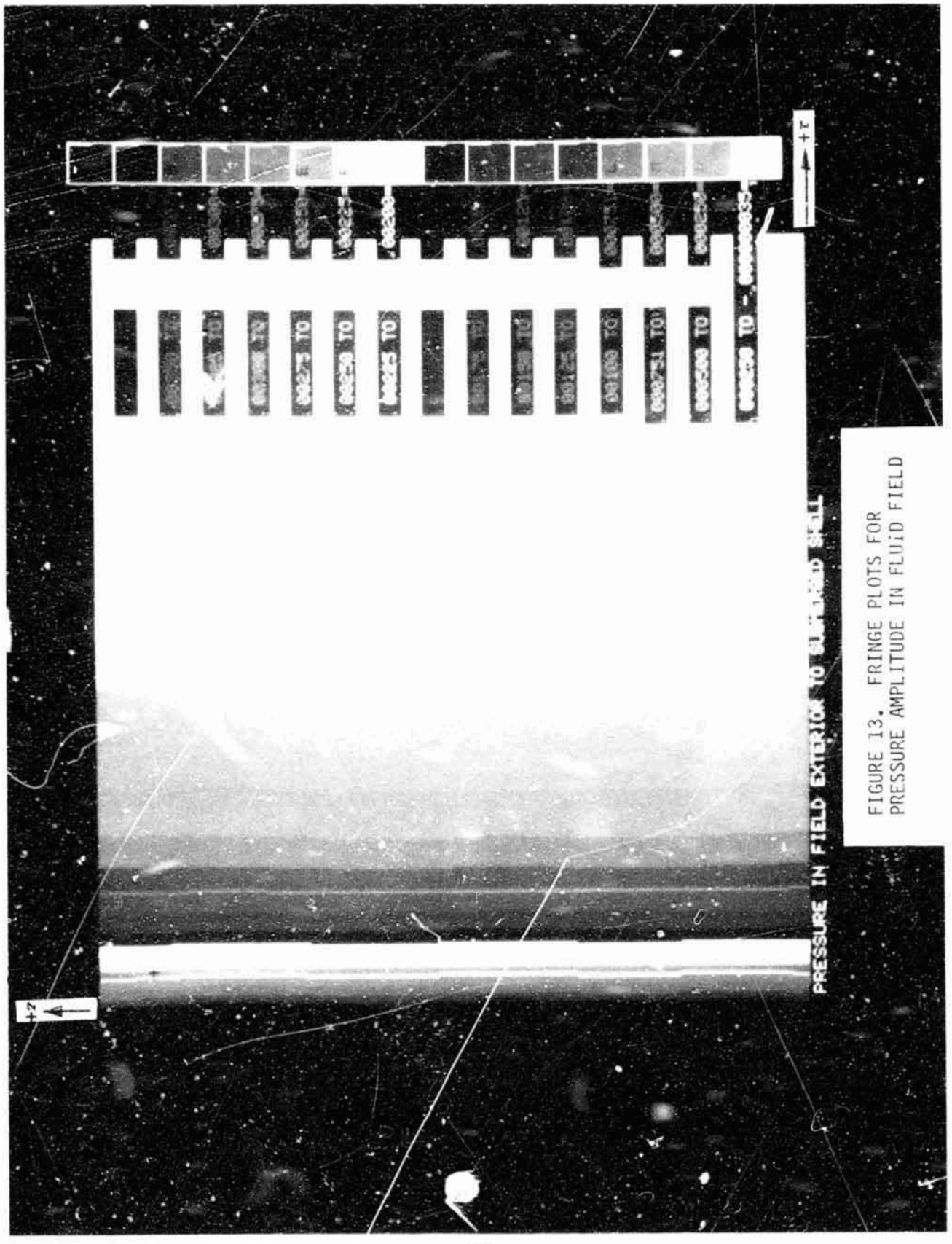

FIGURE 13. FRINGE PLOTS FOR PRESSURE AMPLITUDE IN FLUID FIELD

REFERENCES

1. Flügge, W., Stresses in Shells, Springer-Verlag, 1962.

2. Junger, M. C., and Feit, D., Sound, Structures, and Their Interaction, MIT Press, Cambridge, 1972.

3. Kalinowski, A. J., and Nebelung, C. W., "Solution of Axisymmetric Fluid Structure Interaction Problems", Tenth NASTRAN User's Colloquium, NASA Conference Publication 2249, May 1982.

4. Midlin, R. D., "Influence of Rotary Inertia and Shear on Flexural Motions of Isotropic, Elastic Plates", Journal of Applied Mechanics, March 1951.

5. Abramowitz, M., and Stegun, I. A., Handbook of Mathematical Functions, National Bureau of Standards, June 1964.

6. Zienkiewicz, O. C., The Finite Element Method, (3rd Edition), McGraw-Hill Book Company, 1977.

7. Pica, A., and Hinton, E., "Transient and Pseudo-Transient Analysis of Mindlin Plates", International Journal for Numerical Methods in Engineering, Vol. 15, 1980.

8. Cook, R. D., "Remarks About Diagonal Mass Matrices", International Journal for Numerical Methods in Engineering, Vol. 17, 1981.